Environmental challenges in electrification: Traffic-induced non-exhaust $PM_{2.5}$ emissions in Cangzhou, China

Lewen Wang[a,b,c], Like Jiang[d], Pengfei Fan[e], Wei Hao[b,c], Zeyu Zhang[f], Zhiqiang Zhai[e], Lei Yu[e, g, h], Guohua Song[e], Yizheng Wu[e*]

[a] Key Laboratory of Highway Engineering of Ministry of Education, Changsha University of Science & Technology, Changsha, 410114, Hunan, China.
[b] School of Transportation, Changsha University of Science & Technology, Changsha, 410114, Hunan, China.
[c] Hunan Key Laboratory of Smart Roadway and Cooperative Vehicle-Infrastructure Systems, Changsha University of Science & Technology, Changsha, 410114, Hunan, China.
[d] Institute for Transport Studies, University of Leeds, UK.
[e] Key Laboratory of Transport Industry of Big Data Application Technologies for Comprehensive Transport, Beijing Jiaotong University, 3 Shangyuancun, Haidian District, Beijing 100044, China.
[f] The Hong Kong Polytechnic University, Hong Kong, China.
[g] College of Science and Technology, Texas Southern University, 3100 Cleburne Avenue, Houston, Texas 77004, United States.
[h] Shandong Jiaotong University, Ji'nan 250357, China.

*Corresponding author at:
Yizheng Wu: Beijing Jiaotong University, 3 Shangyuancun, Haidian District, Beijing 100044, China. Email address: wuyizheng@bjtu.edu.cn.

Abstract

Non-exhaust $PM_{2.5}$ emissions are often overlooked despite their increasingly significant contribution. Including non-exhaust emissions to establish a complete road emissions inventory is critical for formulating effective control strategies and reducing health risks especially during the fleet electrification process. This study developed a $PM_{2.5}$ emission estimation framework incorporating exhaust and non-exhaust sources, validated by roadside $PM_{2.5}$ concentrations from a mobile cruise sensing system in Cangzhou, China. The results found that traffic-related $PM_{2.5}$ concentrations contributing to roadside environments exhibit hourly variations, with an average proportion of 44.05%. Analysis of peak-hour $PM_{2.5}$ emissions revealed the non-exhaust sources dominate (91.38%). Under scenarios with 35%, 50%, 75%, and 100% electrification rates, $PM_{2.5}$ emissions will decrease by 6.96%, 11.01%, 17.77%, and 24.53%, respectively, compared to the baseline. This study highlights that fleet electrification will not completely eliminate $PM_{2.5}$ emissions, and helps identify priorities and develop targeted emission control policies for medium-sized populous cities in developing countries.

Keywords: Emission modeling; Traffic-related $PM_{2.5}$ emissions; Mobile monitoring system; Non-exhaust emissions; Electric vehicles

1. Introduction

$PM_{2.5}$ has become a significant public health threat, listed among the top ten causes of premature mortality globally and accounting for over 60% of all air pollution-related deaths (Soleimani et al., 2022). The WHO reports that $PM_{2.5}$ pollution leads to over 90% of the global population living above the safety threshold (10 μg/m^3). Recent urban $PM_{2.5}$ source analyses have identified vehicular $PM_{2.5}$ emissions as a major contributor, particularly in developing countries. Evidence from cities in developed countries, such as New York and Boston in USA and Hamburg in Germany, shows 16%, 25% and 18% contribution respectively (Masri et al., 2015; Masiol et al., 2017; Ramacher et al., 2020). In cities in developing countries such as Shanghai, Beijing and Shenzhen in China and Delhi in India, the percentages are much higher at 39.8%, 45%, 41% and 34.6% respectively (SZMEEB, 2015; Wang et al., 2016; BJMEEB, 2018; Philip K. Hopke, 2022; Zhang et al., 2024).

Vehicle fleet electrification has become a pivotal strategy for mitigating such pollution and health impacts in developing countries, as exemplified by India's FAME-II initiative and China's NEV Industry Development Plan (2021-2035). However, these policies predominantly target exhaust emissions, while overlooking non-exhaust $PM_{2.5}$ emission sources including road dust resuspension, brake wear, tire wear, and road wear. These sources can impact water systems, the environment, and public health (Liu et al., 2022b), representing an emerging environmental challenge that requires urgent attention. Some research has confirmed that non-exhaust $PM_{2.5}$ emissions outweigh exhaust emissions and are becoming a key component of ambient particulate matter pollution (Amato et al., 2014; Matthaios et al., 2022). Moreover, $PM_{2.5}$ non-exhaust emission factors exhibit vehicle load-dependency. Due to their additional battery weight, electric vehicles (EVs) tend to generate higher non-exhaust emission factors than their internal combustion engine vehicles (ICEVs) counterparts (Liu et al., 2022a), and the proportion of $PM_{2.5}$ originating from non-exhaust emissions will continue to rise (Timmers and Achten, 2016). This has raised concerns that the widespread use of EVs may not lead to a significant reduction in $PM_{2.5}$ emissions or air quality benefits (Soret et al., 2014; Hooftman et al., 2018). Evidence from UK, Liu et al. (2024) projected a slight increase in total $PM_{2.5}$ emissions by 2040 under the banning ICEV sales. Until recently, non-exhaust emissions have gained attention. The Euro 7 emission standards pioneer the regulatory initiative to establish controls on non-exhaust $PM_{2.5}$ emissions, specifically encompassing particulate matter from both brake wear and tire wear. China's upcoming China VII emission standards are also planned to address non-exhaust $PM_{2.5}$ emissions. Given that non-exhaust emissions have not yet been widely prioritized and effectively regulated (Fussell et al., 2022), conducting emission assessments under different EVs penetration scenarios is critical for informing the next phase of pollution control measures.

Another challenge is that many countries rely on regulatory fixed-site measurements for ambient air quality monitoring, however, their coverages are often spatially sparse (Tian et al., 2023) or even completely lacking in some developing countries (Apte et al., 2017) due to substantial costs. This limited monitoring coverage fails to capture the spatio-temporal variation characteristics of air pollution, and can lead to underestimation of roadside $PM_{2.5}$ exposure levels and related health impacts (Yu et al., 2022). Moreover, there are increasing numbers of people, particularly vulnerable groups in developing countries, residing near roadsides and exposed to high level of pollution (Kendrick et al., 2015; Wang et al., 2025). Such land use changes can lead to increasing inequalities in pollution burdens and raise further environmental justice challenges, which highlights the need to develop a road network $PM_{2.5}$ emissions estimation method as an alternative approach to address gaps in monitoring networks.

However, existing studies on quantifying road network $PM_{2.5}$ emissions in developing countries are still relatively scarce, especially studies focusing on medium-sized cities, while such cities account for a significant proportion of the population and may develop faster than major urban agglomerations (Berdegué and Soloaga, 2018; J. Liu et al., 2024), playing an important role in reducing public health impacts and achieving environmental justice (Wang et al., 2025). Moreover, existing research on road network emissions calculation typically fails to incorporate non-exhaust emissions, and the calculation results often lack real monitoring concentration data for verification (Rowangould, 2015; Salva et al., 2021; Ratanavalachai and Trivitayanurak, 2023). This may underestimate $PM_{2.5}$ emissions and provide inaccurate emission inventories, making it difficult to support the implementation of customized control measures and promote environmental justice.

To address the knowledge gap mentioned above, our study makes the following key contributions:

1. A method has been developed to estimate $PM_{2.5}$ emissions from road networks, incorporating both exhaust and non-exhaust sources. And the method was validated using a mobile monitoring system with taxi cruising.

2. The road networks $PM_{2.5}$ emission characteristics of medium-sized cities in developing countries was analyzed, using Cangzhou, China as an example. A complete emission inventory was established to quantify the proportion of traffic-related $PM_{2.5}$ emissions in roadside environments. This involved the contribution of each emission component. And The results provide critical data support for formulating next-stage air quality improvement strategies.

3. The $PM_{2.5}$ emission patterns under varying fleet electrification scenarios were portrayed. The results emphasize the importance of regulating non-exhaust $PM_{2.5}$ emissions in the electrification era.

2. Materials and methods

2.1. Study area

This research was conducted using Cangzhou as a case study. Specifically, as shown in **Figure 1(a)**, Cangzhou is located in the Beijing-Tianjin-Hebei region of northern China and has a urban population of 810,000 according to the Tabulation on 2020 China population census by county. It represents a typical medium-sized populous city in developing countries (cities with populations between 500,000 and 1 million are classified as medium-sized cities). The study area covers the two central districts of Cangzhou, and the road network distribution characteristics are shown in **Figure 1(b)**. The heavy-duty truck-permitted principal arterials are mainly located on the periphery, connecting suburban and rural areas. The urban core's road network is predominantly composed of heavy-duty truck-restricted principal arterials and minor arterials.

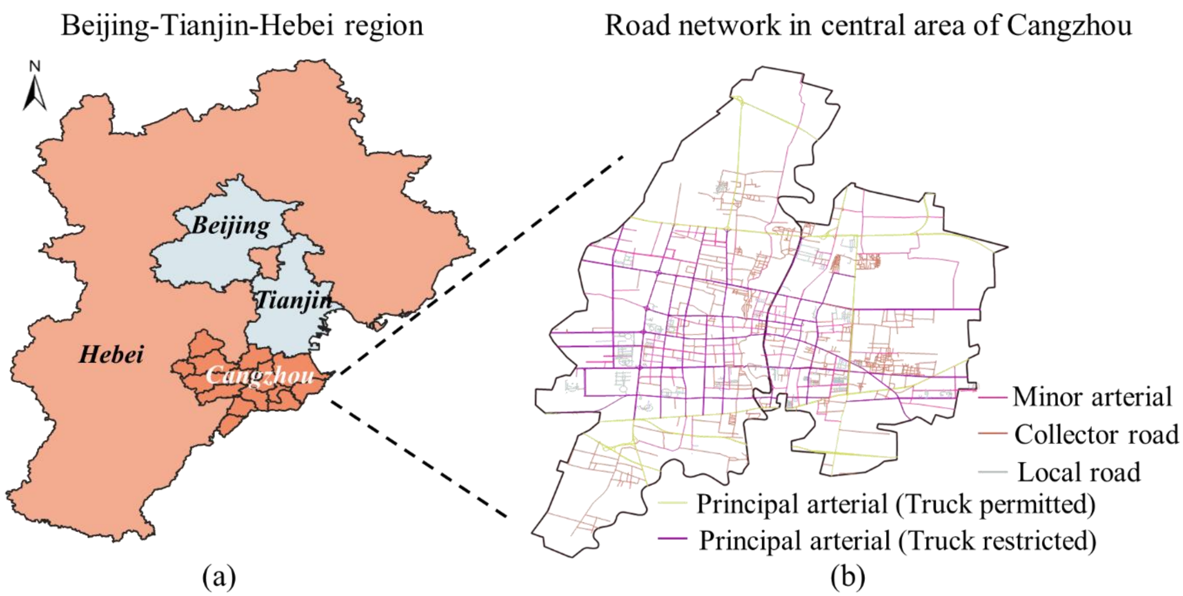

Figure 1 Information about study area. (a) The location Cangzhou in Beijing-Tianjin-Hebei region and. (b) The road network (data source: OpenStreetMap).

2.2. Data collection

2.2.1. Source of road network speed data

The road network link-level speed data was collected by floating car. By installing GPS devices on vehicles, real-time positional data are recorded and integrated with digital road maps to obtain key parameters including date, time, road link ID, link length, and travel time, enabling calculation of average travel speeds within specific time intervals. This study utilized floating car data in 2019 in Cangzhou, with daily datasets reaching millions of records.

2.2.2. Source of traffic flow and vehicle fleet configuration data

The vehicle fleet configuration by emission standard in Cangzhou is shown in **Figure 2(a)**. Taking light-duty passenger vehicles (LDPVs) as an example, in 2019, the proportion of vehicles meet Pre-China I, China I to China VI were 0.01%, 1.79%, 3.7%, 15.5%, 40.8%, 29.8%, and 8.4%, respectively. The data about traffic flow and vehicle type were obtained through field surveys. Specifically, we conducted a two-week field investigation with multiple monitoring sites across different road types in Cangzhou. The traffic flow data collection at each site was carried out by two staff members working in hourly shifts and recording vehicle classification counts at one-minute intervals (**Figure 2(b)**), and more details can be seen in the **Supplementary Materials**. Due to heavy-duty truck restrictions in Cangzhou's central area, the proportion of vehicle types is divided into Heavy-duty truck permitted and restricted scenarios. As **Figure 2(c)** illustrates, the proportions of light-duty passenger vehicles (LDPVs), heavy-duty passenger vehicles (HDPVs), light-duty trucks (LDTs), and heavy-duty trucks (HDTs) for the truck permitted scenario are 78.69%, 1.06%, 12.77%, and 7.48%, respectively. The proportions of LDPVs, HDPVs, and LDTs for the truck restricted scenario are 95.96%, 2.98%, and 1.06%. The electrification rate by vehicle types according to field surveys are as follows: LDPVs (11.97%), HDPVs (27.38%), and LDTs (1.91%), while HDTs are still primarily ICEVs (see **Figure 2(d)**).

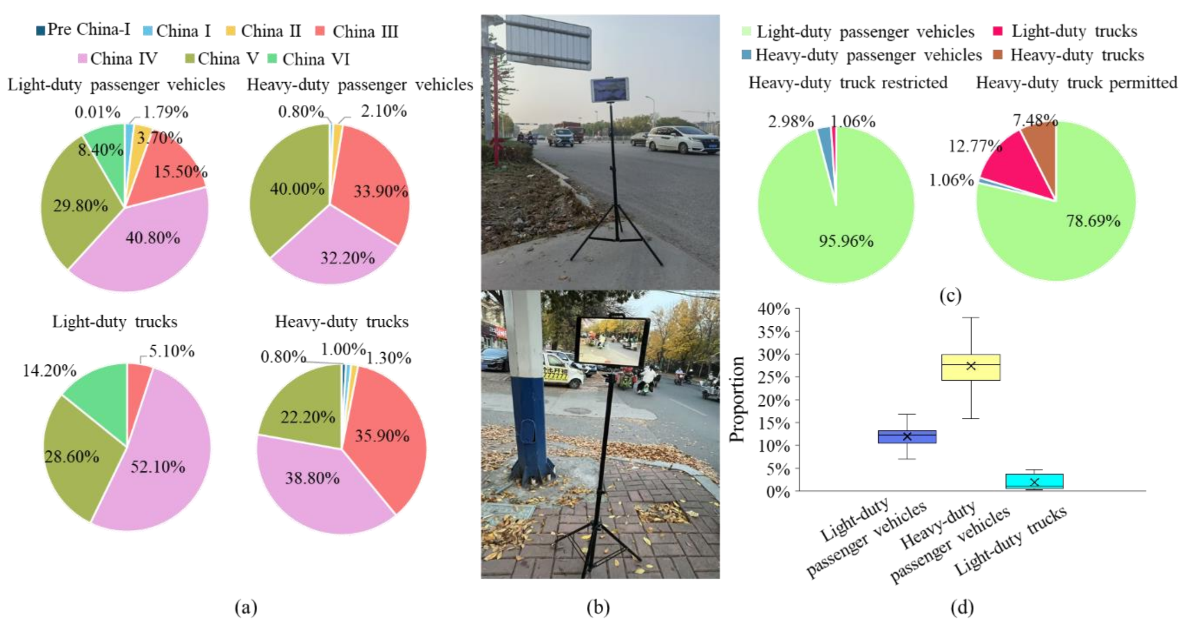

Figure 2 Vehicle fleet configuration in Cangzhou. (a) By emission standards. (b) Field surveys. (c) By road types. (d) Percentage of fleet configuration electrification.

2.2.3. Source of $PM_{2.5}$ emission factors

The emission factors (EFs) comprise non-exhaust and exhaust components. The exhaust EFs were derived from an integrated database developed through Portable Emission Measurement System (PEMS). As shown in **Figure 3 (a)**, comprehensive testing has been conducted over the years, covering LDPVs, HDPVs, LDTs and HDTs. The tested vehicles represent China's all current emission standards. By integrating extensive vehicle trajectory data, an integrated dataset of operating conditions and emissions based on Vehicle Specific Power (VSP) distribution was developed, ultimately establishing a localized exhaust EFs database categorized by road type, speed bin, vehicle type and emission standard. More relevant details can be found in the **Supplementary Materials**.

The non-exhaust EFs for resuspension dust and the wear of brake, tire and road were calculated by applying the widely used estimation model (Beddows and Harrison, 2021; Liu et al., 2021; Lin et al., 2022; Tomar et al., 2022). The specific formulation is shown in **Equation (1)**.

$$\begin{cases} EF = b \times W_{ref}^{\frac{1}{c}} \\ W_{ref} = W/1000 \end{cases} \quad (1)$$

Where EF represents non-exhaust EFs, $mg^{-1}km^{-1}veh^{-1}$; b and c are fitting parameters obtained by the research of Beddows and Harrison (2021), and different types of non-exhaust EFs have different values, specific values shown in **Table S1** in **Supplementary Materials**; W is the vehicle load, kg.

2.2.4. Source of roadside $PM_{2.5}$ concentrations

To validate the results of emission calculations, we measured actual $PM_{2.5}$ concentrations in roadside environments for comparison. A mobile monitoring method integrated with taxi cruising was applied (shown in **Figure 3 (b)**). The system was equipped with laser particle sensors based on laser diffraction theory, with four sensors installed at the taxi's headlight positions for cross-validation and to ensure data validity. The system features a positioning accuracy of better than 20 meters through its dual-mode (GPS+BeiDou) functionality. And it can transmit timestamped data including coordinates and $PM_{2.5}$ concentrations at 3-second intervals. Prior to field deployment, the system underwent comprehensive calibration through material upgrades and shock-absorbing screw installation to minimize measurement errors. The collected dataset was validated by three fixed monitoring stations in Cangzhou using five statistical metrics, with the correlation coefficient (R) exceeding 0.95, and this work has been made publicly available (Wu et al., 2020). More details can be seen in **Supplementary Materials**. In 2019, a fleet of 49 taxis was deployed to collect roadside $PM_{2.5}$ concentration data, with over 10 million data collected each season.

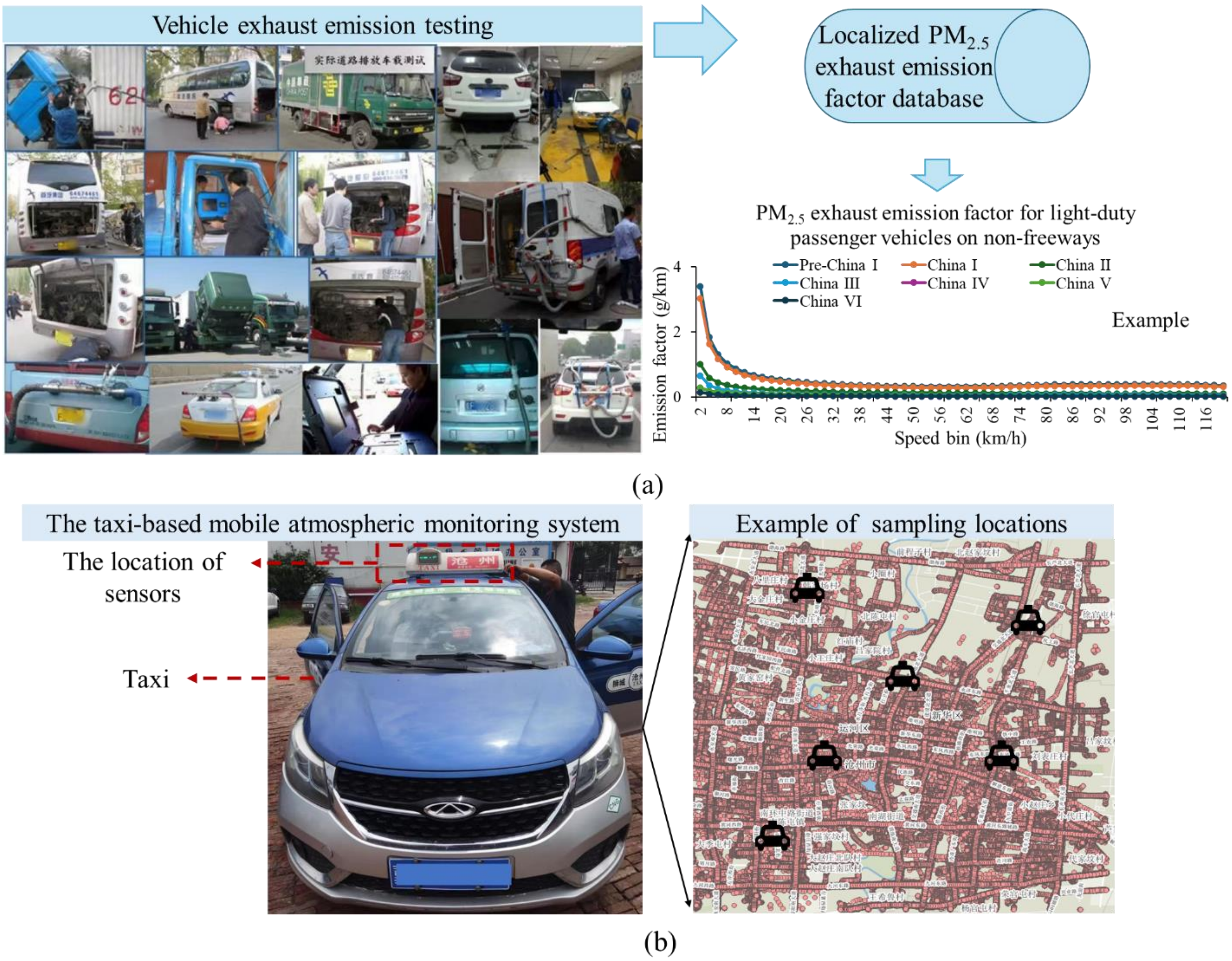

Figure 3 $PM_{2.5}$ emission factors and roadside concentration monitoring. (a) The vehicle exhaust emission testing and database of localized $PM_{2.5}$ exhaust emission factors. (b) The mobile monitoring system and the sampling examples.

2.3. Calculation method for $PM_{2.5}$ emissions from road network

Figure 4 illustrates the steps for road network $PM_{2.5}$ emission estimation in this study. Step 1: establishing traffic flow models and using floating car speed data to obtain link-level traffic flow. Step 2: calculating vehicle-specific flow based on emission types, vehicle types, and electrification rates. Step 3: computing exhaust and non-exhaust EFs for different scenarios. Step

4: calculating the total emissions. Step 5: verifying the reliability of emission calculations. The details are detailed in the following sections.

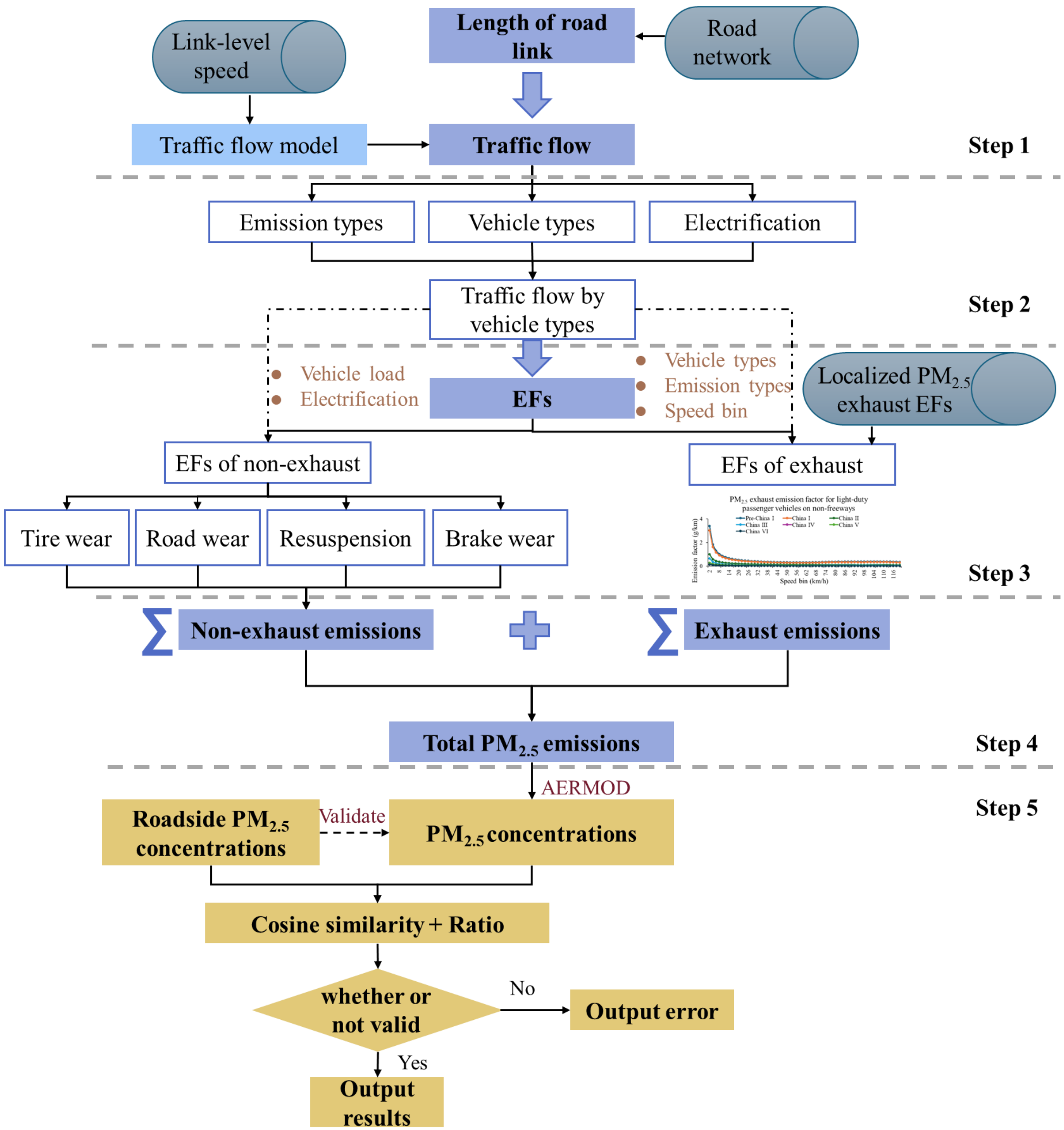

Figure 4 The framework for $PM_{2.5}$ emissions from road networks.

2.3.1. Traffic flow models

Link-level traffic speed and flow data are key for estimating network emissions. However, obtaining large-scale, link-level flow data is challenging due to the high cost and sparse coverage of traffic detectors on the road network (Liu et al., 2019). Many cities already employ floating car systems, which make collecting link-level speed data relatively straightforward (Houbraken et al., 2018; Sunderrajan et al., 2016; Xu et al., 2013). Consequently, utilizing real-time link speed data as input to traffic flow models has become a common method for estimating traffic flow, and is widely adopted in road network emission calculations (Chen et al., 2022; Jiang et al., 2021; Pan et al., 2024; Zang et al., 2022; Zhao et al., 2009).

The Underwood and Van Aerde models are two widely used traffic flow models, with their formulas shown in **Equations (2)** and **(3)**, respectively. The Van Aerde model is applicable to various traffic conditions and road types, and the Underwood model is better suited for traffic flow on urban principal arterials and minor arterials (Zang et al., 2022). After a comparative analysis of multiple traffic flow models, the Van Aerde model was selected to characterize traffic flow relationships on principal arterials (truck permitted), while the Underwood model was applied to both principal arterials (truck restricted) and minor arterials in our study. The details and the model parameter calibration results can be seen in the **Supplementary Materials**.

$$\begin{cases} \rho = \dfrac{1}{c_1 + \dfrac{c_2}{v_{free} - v} + c_3 v} \\ c_1 = v_{free}(2v_m - v_{free}) / \rho_j v_m^2 \\ c_2 = v_{free}(v_{free} - v_m)^2 / \rho_j v_m^2 \\ c_3 = 1 / q_c - v_{free} / \rho_j v_m^2 \end{cases} \tag{2}$$

$$v = v_{free} e^{-\frac{\rho}{\rho_m}} \tag{3}$$

Where ρ is the density of traffic flow; ρ_j is the blocking density; v_m is the critical speed, defined as the speed at which road flow reaches its capacity; v_{free} is the free flow speed; c_1, c_2, c_3 are intermediate variables; v is the speed of traffic flow; q_c is the capacity; ρ_m is the density at the capacity.

2.3.2. Calculation for different vehicle type traffic flow

After obtaining the link-level traffic flow, the traffic flow data for different vehicle types on different roads are calculated by using **Equation (4)**.

$$\begin{cases} Q_{r,n}^{g} = Q_{r,n} \times \lambda_g \\ q_g^{r,n,Green} = Q_{r,n}^{g} \times Green_g \\ q_{g,k}^{r,n} = \lambda_k \times (Q_{r,n}^{g} - q_g^{r,n,Green}) \end{cases} \tag{4}$$

Where $Q_{r,n}$ is the total traffic flow on the *n*th link of road type *r*, calculated using the established traffic flow model, pcu/h; $Q_{r,n}^{g}$ is the total traffic flow for vehicle type *g* on the *n*th link of road type *r*, pcu/h; λ_g is the proportion of vehicle type *g*; $Green_g$ is the electrification rate of vehicle type *g*; λ_k is the proportion of emission standard *k*.

2.3.3. Method for $PM_{2.5}$ emission factors

EFs are calculated separately for EVs and ICEVs. Specifically, exhaust EFs for ICEVs are derived from the localized database and computed based on vehicle types, emission standards, road types, and speed intervals, while non-exhaust EFs are calculated according to vehicle weight for different vehicle types using **Equation (1)**. The total EFs are calculated as **Equation (5)**.

$$EF_{icev}^{g,k,r,v} = (EF_{tyre}^{g} + EF_{road}^{g} + EF_{resus}^{g} + EF_{brake}^{g}) \times 10^{-3} + EF_{emission}^{g,k,r,v} \tag{5}$$

Where $EF_{icev}^{g,k,r,v}$ is the total EFs for ICEV of type *g* with emission standard *k* at speed bin *v* on road type *r*, g/km; $EF_{emission}^{g,k,r,v}$ is the exhaust EFs for ICEV of type *g* with emission standard *k* at speed bin *v* on road type *r*, g/km; EF_{tyre}^{g}, EF_{road}^{g}, EF_{resus}^{g} and EF_{brake}^{g} are non-exhaust EFs for tire wear, road wear, dust resuspension, and brake wear, respectively, mg/km.

ICEVs converted to equivalent EVs will experience weight increase due to battery systems, and numerous studies have quantified electrification-induced weight changes by comparing EVs and ICEVs of the same make and model with matched engine specifications. As summarized in **Table 1,** the weight increase ranges from 16% to 24%. Thus, this study examines weight increments of 16%, 17%, 18%, 19%, 20%, 21%, 22%, 23%, and 24% for EVs compared to ICEVs and calculates non-exhaust EFs based on vehicle weight by types. Moreover, ICEVs decelerate wheels by mechanical braking systems, generating particulate emissions through friction. EVs employ a combined friction and regenerative braking approach, where regenerative braking decelerates without friction and thus no particulate emissions (Barlow, 2014). The $PM_{2.5}$ emissions from brake wear in EVs are usually calculated using a proportional method (Beddows and Harrison, 2021; Liu et al., 2021, 2022a), as shown in **Equation (6)**.

$$EF_{bev}^{g} = (EF_{tyre}^{g'} + EF_{road}^{g'} + EF_{resus}^{g'} + \alpha \times EF_{brake}^{g'}) \times 10^{-3} \qquad (6)$$

Where EF_{bev}^{g} is the total EFs for EV of type *g*, g/km; α is the proportion of mechanical braking in EVs, with our study specifically adopting the values of 0.1, 0.3, 0.5, and 0.7 from the range summarized in **Table 1** for analysis; $EF_{tyre}^{g'}$, $EF_{road}^{g'}$, $EF_{resus}^{g'}$ and $EF_{brake}^{g'}$ are non-exhaust EFs for EVs of tire wear, road wear, dust resuspension, and brake wear, respectively, mg/km.

Table 1 Research about the weight changes after vehicle electrification and the mechanical braking ratio α value.

References	Weight changes	α
Liu et al. (2022a)	The equivalent EV weight increased by 23% for gasoline vehicles.	0.42, 1 (0% and 68% regenerative braking)
	The equivalent EV weight increased by 18% for diesel vehicles.	
Faria et al. (2012)	The equivalent EV weight increased by 20% for ICEV.	/
Liu et al. (2021)	The equivalent EV weight increased by 20% for ICEV.	0, 0.5, 1
Timmers and Achten (2016)	The equivalent EV weight increased by 24% for ICEV.	/
Beddows and Harrison (2021)	The equivalent EV weight increased by 23.57% for gasoline vehicles.	0, 0.1, 1
	The equivalent EV weight increased by 16.58% for diesel vehicles.	
	The equivalent EV weight increased by 21% for ICEV.	

2.3.4. Methods for $PM_{2.5}$ emissions

The total $PM_{2.5}$ emissions of the road network are composed of emissions from ICEVs and EVs, as shown in **Equation (7)**.

$$E = E_{icev} + E_{bev} \tag{7}$$

Where E is the total emissions, g/h; E_{icev} is the emissions from ICEVs, g/h; E_{bev} is the emissions from EVs, g/h.

Specifically, the calculation of emissions from ICEVs is shown in **Equation (8)**.

$$\begin{aligned} E_{icev} &= E_{icev}^{emission} + E_{icev}^{no-emission} = \sum_{r,n}\sum_{g}\sum_{k} L_{r,n} \times q_{g,k}^{r,n} \times EF_{icev}^{g,k,r,v} \\ &= \sum_{r,n}\sum_{g}\sum_{k} L_{r,n} \times q_{g,k}^{r,n} \times EF_{emission}^{g,k,r,v} + \sum_{r,n} L_{r,n} \times \sum_{g} q_{g,k}^{r,n} \times (EF_{tyre}^{g} + EF_{road}^{g} + EF_{tresus}^{g} + EF_{brake}^{g}) \times 10^{-3} \end{aligned} \tag{8}$$

Where $E_{icev}^{emission}$ and $E_{icev}^{no-emission}$ is exhaust emissions and non-exhaust emissions of ICEVs, respectively, g/h; $L_{r,n}$ is the length of nth link for road type r, km; $q_{g,k}^{r,n}$ is the ICEV traffic flow of vehicle type g with emission standard k on the nth link of road type r, pcu/h.

The calculation of emissions from EVs is shown in **Equation (9)**.

$$\begin{aligned} E_{bev} &= \sum_{r,n}\sum_{g} L_{r,n} \times q_{g}^{r,n,Green} \times EF_{bev}^{g} \\ &= \sum_{r,n}\sum_{g} L_{r,n} \times q_{g}^{r,n,Green} \times (EF_{tyre}^{g'} + EF_{road}^{g'} + EF_{resus}^{g'} + \alpha \times EF_{brake}^{g'}) \times 10^{-3} \end{aligned} \tag{9}$$

Where $q_{g}^{r,n,Green}$ is the EV traffic flow for vehicle type g of the nth link for road type r, pcu/h.

2.3.5. Methods for validation

AERMOD is a widely used atmospheric dispersion modeling method with good applicability and reliability (Rowangould, 2015; Ratanavalachai and Trivitayanurak, 2023). We utilized AERMOD to simulate the dispersion of road network $PM_{2.5}$ emissions for obtaining concentration values. Then, verify the results by comparing the actual measured concentration values from the taxi-based mobile sensing system. And two indicators including cosine similarity and ratio were used to evaluate hourly variation trends and magnitude relationships, as presented in **Equation (10)** and **Equation (11)**.

$$\cos(\boldsymbol{w}_{\text{real}}^{s}, \boldsymbol{w}_{\text{road network}}^{s}) = \frac{\boldsymbol{w}_{\text{real}}^{s} \cdot \boldsymbol{w}_{\text{road network}}^{s}}{\left\| \boldsymbol{w}_{\text{real}}^{s} \right\| \times \left\| \boldsymbol{w}_{\text{road network}}^{s} \right\|} = \frac{\sum_{y=1}^{Y} (w_{\text{real}}^{s,y} \cdot w_{\text{road network}}^{s,y})}{\sqrt{\sum_{y=1}^{Y} {w_{\text{real}}^{s,y}}^{2}} \times \sqrt{\sum_{y=1}^{Y} {w_{\text{road network}}^{s,y}}^{2}}} \tag{10}$$

$$\begin{cases} \eta_y = \dfrac{1}{S} \times \sum_{s=1}^{S} \dfrac{\mathbf{w}_{\text{road network}}^{s,y}}{\mathbf{w}_{\text{real}}^{s,y}} \times 100\% \\ \boldsymbol{\eta} = [\eta_1, \eta_2, \ldots, \eta_y] \end{cases} \tag{11}$$

Where $\cos(\boldsymbol{w}_{\text{real}}^{s}, \boldsymbol{w}_{\text{road network}}^{s})$ is cosine similarity, a metric that quantifies the directional alignment between two vectors in multidimensional space. The value varies between -1 and 1, when values approaching 1 indicate strong vector similarity, values nearing -1 represent diametric opposition, and 0 signifies orthogonal vectors exhibiting no correlation. Vectors $\boldsymbol{w}_{\text{real}}^{s}$ and $\boldsymbol{w}_{\text{road network}}^{s}$ represent the hourly monitoring $PM_{2.5}$ concentrations and the hourly simulated road-network concentrations at location s, respectively. Y is the total number of hours. $w_{\text{real}}^{s,y}$ and $w_{\text{road network}}^{s,y}$ are the actual value and simulated value at the y th hour in the s th location, respectively. S is the total number of locations. η_y is the ratio between the simulated value and the actual monitoring value at hour y; $\boldsymbol{\eta}$ is a vector of different hourly ratios.

3. Results and Discussion

3.1. The validation of emission calculations

Hourly $PM_{2.5}$ emission estimation and dispersion simulation were conducted for the road network from 8:00 to 20:00 by using method in **Figure 4**. A grid-based methodology was employed to validate the road emission calculations. By integrating contemporaneous roadside monitoring data, cosine similarity and concentration ratios were calculated across 90 grid cells

(800 m×800 m each) within the study area. The calculation steps and spatial grid division information are provided in the **Supplementary Materials**.

As shown in **Figure 5(a)**, the monitored and simulated concentrations demonstrate strong agreement in their hourly variations. The cosine similarity in each grid cell exceeded 0.7, with a mean value reaching 0.96. This indicates strong agreement between the concentration trends derived from emission-dispersion modeling and actual roadside measurements, showing the reliability of the method. The results about ratio calculation are presented in **Figure 5(b)**. The findings demonstrate that the concentration contribution of road network $PM_{2.5}$ emissions to total roadside ambient environment varies with hours, which is also confirmed in the study of Li and Managi (2021). The peak ratio is observed during the morning rush hour, reaching 55.97% at 8:00, while the lowest ratio (32.65%) is observed at 12:00. The average hourly ratio of emissions from the road network is 44.05%. The results are reliable as other studies reported that traffic-related sources contribute over 35% to total $PM_{2.5}$ concentrations (Wang et al., 2016; Dabek-Zlotorzynska et al., 2019), reaching 35% to 48% during peak morning hours (Jeong et al., 2019), which is close to the proportion observed in our result. This dynamic ratio also provides a methodological basis for the estimation of $PM_{2.5}$ concentrations in roadside environment by using road network emission-dispersion modeling.

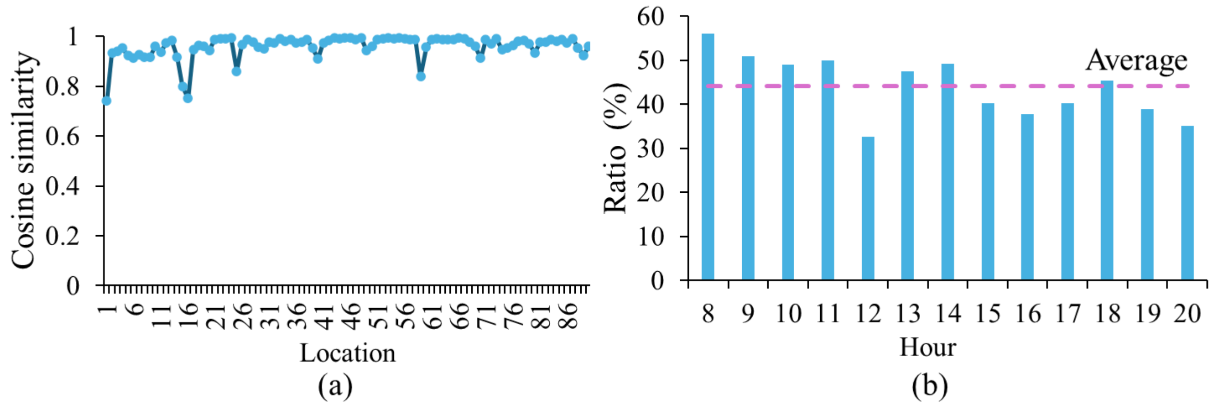

Figure 5 The validation of $PM_{2.5}$ emission calculations. (a) Cosine similarity. (b) Ratio.

3.2. Emission characteristics for different road types

As shown in **Figure 6(b)**, non-exhaust sources represent the dominant contributor to $PM_{2.5}$ emissions. Across various scenarios incorporating EVs weight gains (16%–24%) and α values (0.1, 0.3, 0.5, 0.7), non-exhaust emissions account for over 83%, 97%, and 97% of the total on truck-permitted principal arterials, truck-restricted principal arterials, and minor arterials, respectively. The higher truck share (20.25%) on permitted principal arterials results in a significantly larger proportion of exhaust emissions, exceeding 15% (compared to approximately 2.5% on truck-restricted major roads). As illustrated in **Figure 6(a)**, the highest average hourly $PM_{2.5}$ emissions occur on truck-permitted major roads. Meanwhile, emissions on truck-restricted major roads display greater variability, a pattern attributable to fluctuations in commuter traffic flow. Exposure to $PM_{2.5}$ is epidemiologically associated with adverse health outcomes such as dementia and lung cancer, particularly in roadside environments due to their proximity to the public (Halonen et al., 2016; Chen et al., 2017). **Figure 6(c)** presents the spatial distributions of $PM_{2.5}$ emissions and residential communities, with residential location dataset sourced from Anjuke (www.anjuke.com), a leading Chinese real estate platform (this dataset has been made publicly available in our previous work and can be accessed via this link: https://doi.org/10.1016/j.trd.2025.104762). As visually depicted in **Figure 6(c)**, the residential areas are in close proximity to the road networks. The quantitative results (**Figure 6(d)**) indicate that the majority of residential areas are located within 500m road buffer (99.87%), with 94.07% located within 200m and 70.58% within 100m buffer zones. This spatial characteristic readily leads to heightened resident exposure to non-exhaust $PM_{2.5}$ emissions, which is an increasingly significant yet frequently overlooked source of pollution, presenting a new potential health risk for roadside inhabitants. Furthermore, population living in near-road environments shows an increasing trend, especially vulnerable groups (Kendrick et al., 2015; Rowangould, 2013; Karner and Golub, 2019). This pattern may exacerbate environmental justice concerns and further emphasize the need for a segment-level analysis of $PM_{2.5}$ emission contributions in the road network to guide targeted pollution control.

Moreover, this emission characteristic is influenced by the road network structure of the study area. In medium-sized cities of developing countries, principal arterials account for a higher proportion of the road network, concentrating in central areas and serving as primary traffic corridors (Wang et al., 2019), as shown in **Figure 1(b).** In contrast, some developed cities possess more mature road network structures with higher accessibility (Shi et al., 2019; Wang et al., 2020; Burghardt et al., 2022), where traffic flow distribution could result in relatively even emissions. Some studies have confirmed the road network structure's impact on $PM_{2.5}$ emissions. Research in C. Yu et al. (2023) shows that road network structure accounts for 19.8% of $PM_{2.5}$ concentration. Notably, higher proportions of collector roads and minor arterials are found to reduce $PM_{2.5}$ concentrations (Wang et al., 2017). Our previous Geographically Weighted Regression (GWR) model (Wang et al., 2025) for the study area indicated that roadside $PM_{2.5}$ concentrations were positively associated with industrial areas, truck-permitted principal arterials, and collector roads, but negatively associated with residential areas. This spatial pattern reflects the urban morphology of Cangzhou, a medium-sized city in a developing country, which features well-equipped central areas and a peripheral concentration of industrial zones and freight routes. Such an urban layout may exacerbate inequalities in pollution exposure resulting from $PM_{2.5}$ emissions from the road network. Moreover, even in developed cities like Houston, USA, low-income neighborhoods along industrial corridors experience environmental inequities due to their proximity to freight transit routes (Demetillo et al., 2020). A more detailed discussion is provided in **Section 3.5**. These findings provide valuable insights for optimizing urban planning strategies in cities to mitigate $PM_{2.5}$ emissions from road networks.

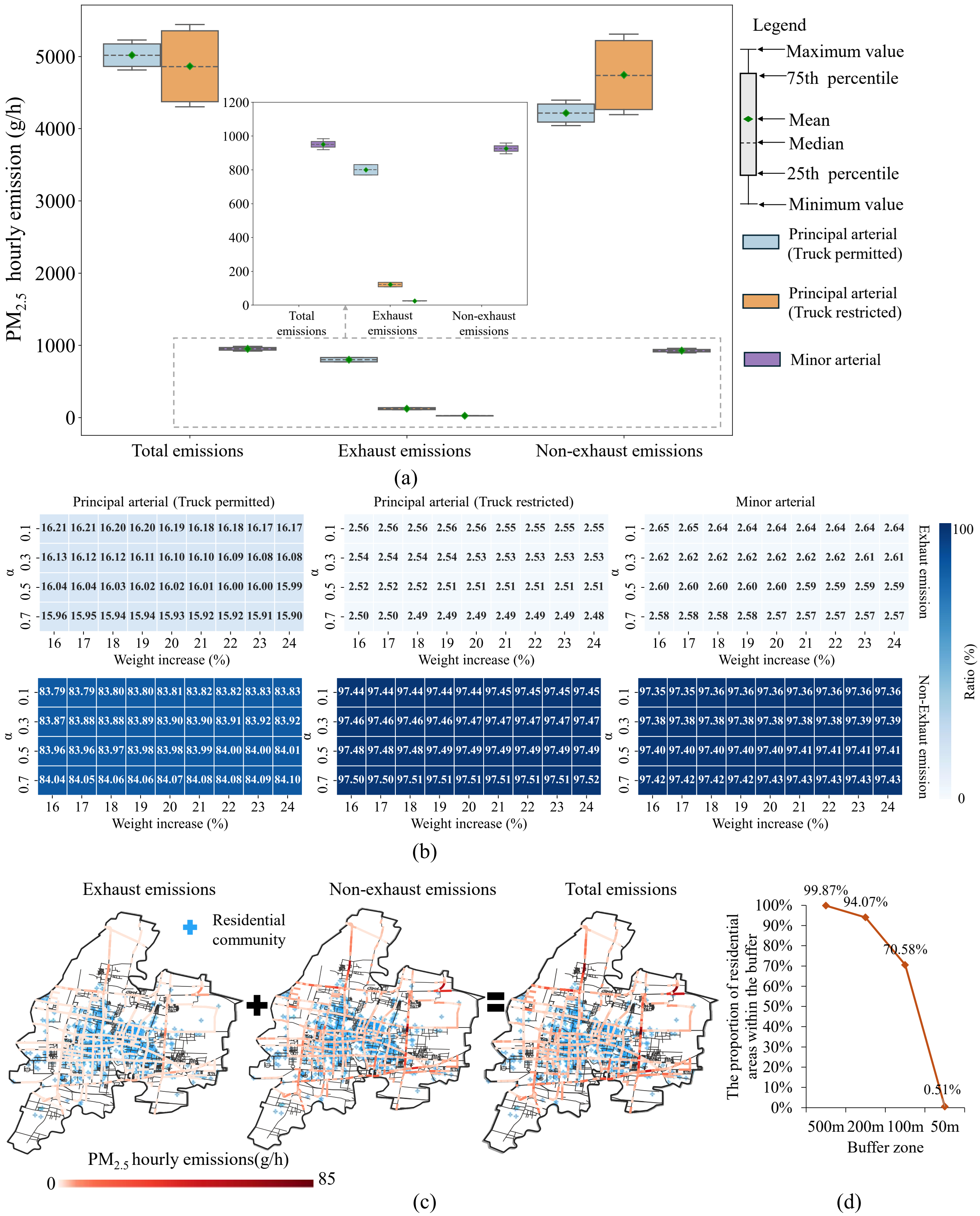

Figure 6 The characteristics of $PM_{2.5}$ emission for different road types. (a) Statistical characteristics. (b) Ratio of exhaust and non-exhaust emissions under different vehicle weight

increases and α values. (c) Spatial distributions. (d) The percentage of residential areas located within different road buffer zones.

3.3. Emissions characteristics by vehicle types

The distribution of $PM_{2.5}$ exhaust emissions across different vehicle types is illustrated in **Figure 7**. Trucks accounted for 87.79% of hourly exhaust emissions, identifying as the primary source. HDPVs contribute 11.09% of the emissions, while LDPVs account for less than 2%. Vehicles meeting China III and IV emission standards remain the dominant contributors to $PM_{2.5}$ exhaust emissions, representing 50.53%, 68.32%, 64.41% and 64.13% among LDPVs, HDPVs, LDTs, and HDTs, respectively. This distribution demonstrates that China's progressively stringent emission standards have effectively controlled vehicular exhaust emissions. Specifically, the China V emission standard (2017) first introduced explicit $PM_{2.5}$ emission limits, while the China VI standard (2019) implemented even stricter controls (MEEC, 2019).

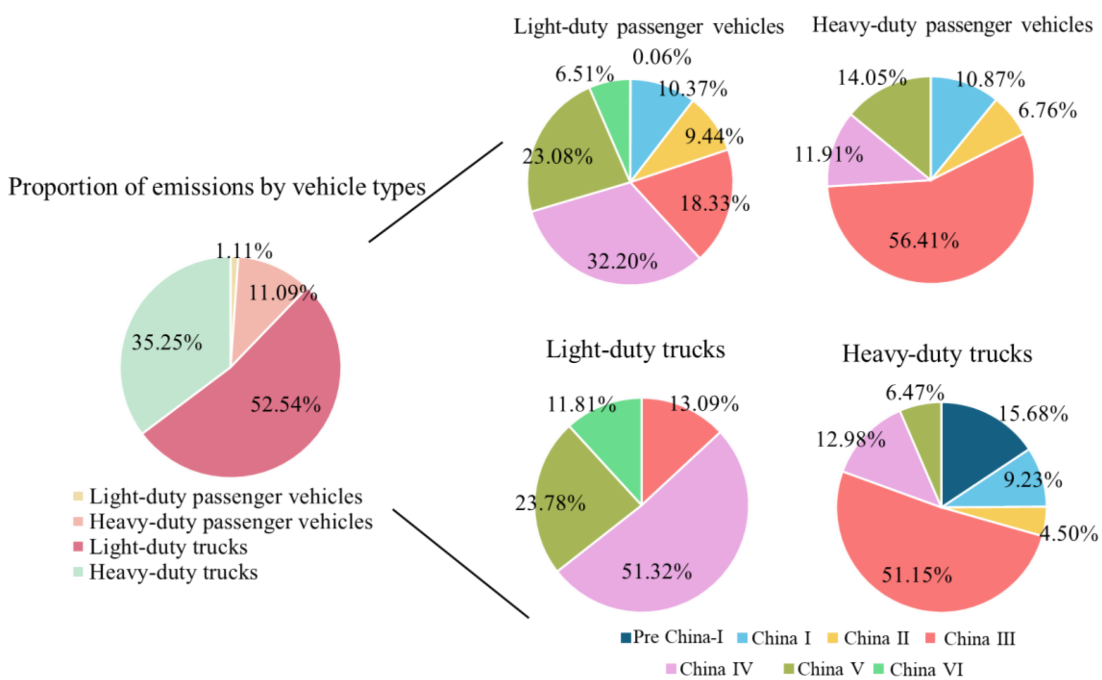

Figure 7 Percentage of $PM_{2.5}$ exhaust emissions by vehicle types.

For individual vehicles, non-exhaust EFs are influenced directly by weight, resulting in higher emissions for HDTs. At the road network level, LDPVs are also key contributors due to their dominant traffic volume. **Figure 8(a)** and **(b)** present the distribution of non-exhaust $PM_{2.5}$ emissions across vehicle types, showing both their overall contributions and their respective shares within the four non-exhaust emission sources. LDPVs emerge as the dominant source, responsible for 75.79% (mean value) of total non-exhaust emissions. Notably, electrified LDPVs, representing 12% of the current vehicle fleet configuration, already account for 9.36% (mean value) of non-exhaust emissions. This reveals an emerging concern: while exhaust emissions have been effectively controlled through stringent emission standards, the accelerating fleet electrification is expected to further increase non-exhaust emissions. The growing adoption of EVs may not lead to significant $PM_{2.5}$ reduction. As Hooftman et al. (2018) proposed, EVs may bring more non-exhaust emissions, indicating that switching to EVs cannot lead to substantial reductions in $PM_{2.5}$ pollutions. Traffic-related $PM_{2.5}$ emissions remain a critical environmental and public health challenge.

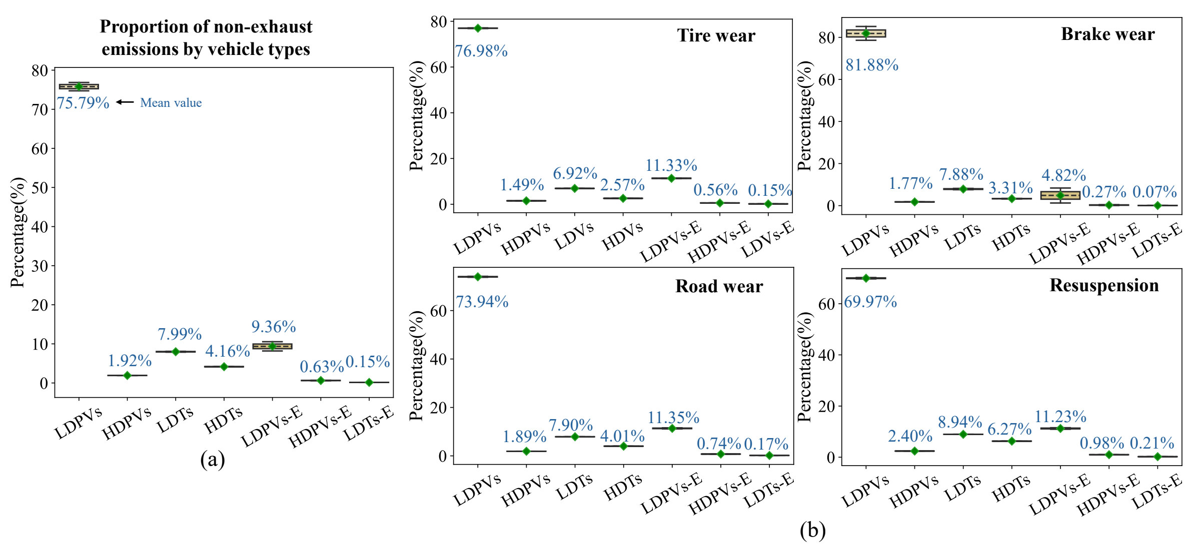

Figure 8 Percentage of $PM_{2.5}$ non-exhaust emissions by vehicle types. (a) The overall contributions. (b) Respective shares within the four non-exhaust emission sources.

3.4. Non-exhaust $PM_{2.5}$: a critical emission source

Figure 9 illustrates the proportional characteristics of $PM_{2.5}$ emissions across different components during peak hours. $PM_{2.5}$ exhaust emissions account for only about 8.62% (mean value), while non-exhaust emissions contribute 91.38%, showing a growing share in total traffic-related emissions. This pattern is also common in many countries (see **Table 2**). Research from seven European countries indicates that non-exhaust emissions have become the dominant source of road $PM_{2.5}$ (Lewis et al., 2019). Data from the UK national emission inventory shows a sharp increase in the contribution from tire, brake, and road wear, which rose from 26% in 2000 to 60% in 2016 (Lewis et al., 2019). The US National Emissions Inventory data reveal that non-exhaust emissions have constituted over 80% of road traffic emissions since 2015, with their share projected to reach 97% by 2030 (OECD, 2020). Research by Piscitello et al. (2021) further demonstrates that non-exhaust sources may be the primary contributor, accounting for over 90% of total traffic-related $PM_{2.5}$ emissions.

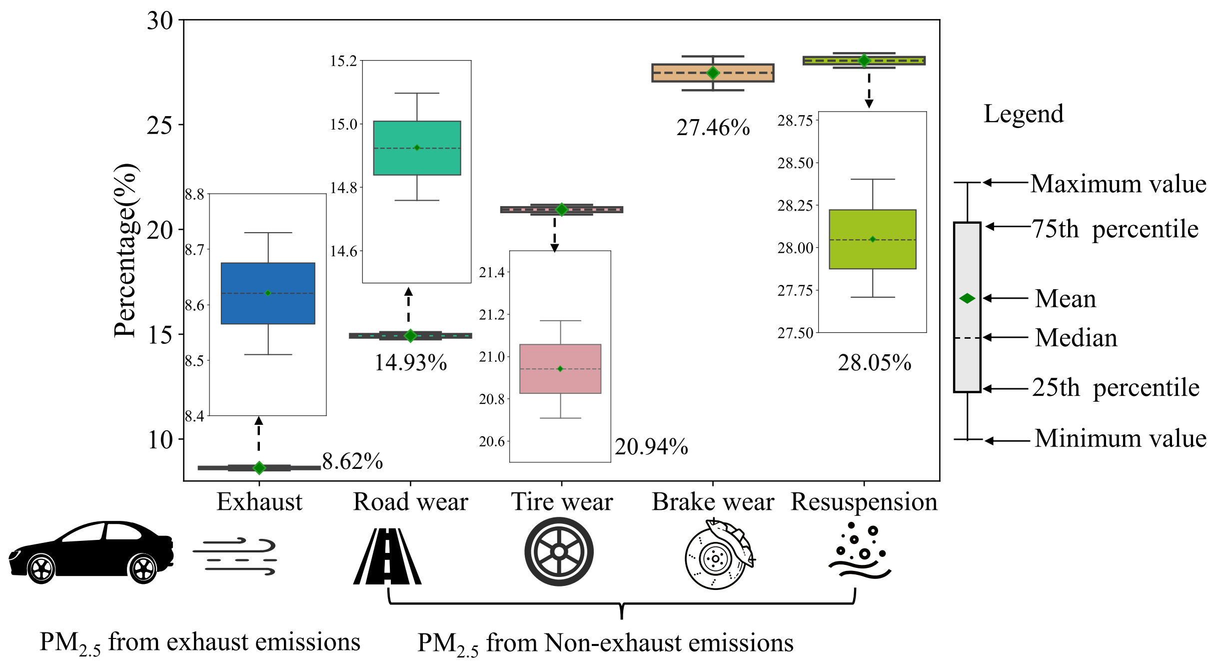

Figure 9 Percentage of each part for hourly $PM_{2.5}$ emission.

Table 2 Some references about road $PM_{2.5}$ emissions.

References	City (Country)	Key points
Lewis et al. (2019)	Seven European countries: the UK, France, Germany, Finland, Denmark, Netherlands, and Sweden.	All countries exhibit the same pattern: exhaust emissions demonstrate a consistent decline, while non-exhaust emissions display an increasing trend and are gradually becoming the dominant source of road $PM_{2.5}$ emissions.
EEA (2022)	European countries	Non-exhaust emissions (from brake, tire wear, and road abrasion) accounted for 59% of $PM_{2.5}$ emissions from road transport in the EU-27 in 2022.
Lewis et al. (2019)	UK	Exhaust emissions have declined annually, while non-exhaust emissions have increased, constituting a growing share of total $PM_{2.5}$ emissions, rising from 26% in 2000 to 60% in 2016.
OECD (2020)	US	Non-exhaust emissions have constituted over 80% of road traffic emissions since 2015, and their share is projected to increase to 97% by 2030.
Piscitello et al. (2021)	/	Non-exhaust sources account for over 90% of total traffic-related particle matter emissions, becoming the primary contributor.

These findings demonstrate that non-exhaust emissions have emerged as both the primary source and critical control target for future $PM_{2.5}$ mitigation strategies. The proportions for the wear of brakes, roads, tires, and dust resuspension are 27.46%, 14.93%, 20.94%, and 28.05%, respectively (shown in **Figure 9**). Dust resuspension represents the highest proportion, as vehicle movement aerodynamically disturbs surface-deposited $PM_{2.5}$ particles through airflow generation and pressure differentials, causing their re-entrainment into the air. These $PM_{2.5}$ could originate from various sources, including the wear of brake, tire, and road. Research by Lin et al., (2022) also demonstrates that $PM_{2.5}$ resuspension constitutes the predominant sector, with a contribution rate as high as 37%-60%. In a Canada-focused study by Dabek-Zlotorzynska et al. (2019), $PM_{2.5}$ resuspension accounted for approximately 23% of $PM_{2.5}$ emissions. Gummeneni et al. (2011) found a 26% share of $PM_{2.5}$ resuspension in Hyderabad, India. Street cleaning has been identified as an effective way to mitigate $PM_{2.5}$ resuspension, including the use of water or chemical dust suppressants (Piscitello et al., 2021). For example, applying chemical agents like magnesium chloride as dust suppressants, the background $PM_{2.5}$ levels were estimated to decrease by 6-8% (Gulia et al., 2019). Moreover, particulate matter resuspension is more likely to occur on smooth pavement surfaces, and that rough-textured pavements can mitigate this phenomenon (Amato et al., 2016; Gulia et al., 2019).

Brake wear emissions constitute the second-largest contributor (shown in **Figure 9**). During vehicle breaking, particulate matter is generated by friction between the drums and brake pads (Piscitello et al., 2021). Upgrading the materials of brake pads to enhance wear resistance and thermal stability can effectively reduce $PM_{2.5}$ emissions from braking operations (such as titanium coatings) (Razo et al., 2016; Piscitello et al., 2021). Furthermore, brake wear is closely associated with driving behavior, as frequent and aggressive braking significantly increases interfacial temperatures and subsequently increases brake wear emissions (Garg et al., 2000; Kwak et al., 2013; Zum Hagen et al., 2019). Promoting smoother driving habits can be a potential mitigation strategy (Querol et al., 2018; Vojtíšek-Lom et al., 2021; Wei et al., 2022). Optimizing signal control at intersections and applying advanced autonomous driving technologies with predictive braking systems can effectively reduce intense friction braking events (De Coensel et al., 2012; Fussell et al., 2022).

Tire wear and road wear have become major sources of urban $PM_{2.5}$ emissions. Tires are primarily composed of rubber, fibers, carbon black fillers, and other materials. Road surfaces are mainly categorized into asphalt and concrete pavements. Friction between tires and road surfaces causes tire materials to fracture under stress, and the rolling of tires peels off pavement materials, both releasing particles in the process. Optimizing materials or structures can help minimize emissions from tire wear and road wear. For example, adding rubber crumbles to asphalt mixtures, adopting double-layer porous asphalt designs or using more wear-resistant tire materials (such as modified silica as an additive) are effective approaches (Bressi et al., 2019; Vieira et al., 2019; Li et al., 2021). Additionally, adopting smoother driving behaviors (e.g., avoiding aggressive deceleration) and maintaining optimal tire pressure and wheel alignment settings are feasible measures (Fussell et al., 2022; Giechaskiel et al., 2024; Liu et al., 2022b).

The Euro 7 emission standards represent a pioneering global effort to regulate non-exhaust $PM_{2.5}$ emissions (all new vehicles sold must comply starting July 1, 2025). The upcoming China VII emission standards mark the first regulatory framework to address non-exhaust $PM_{2.5}$ emissions (mostly for brake and tire wear) in China. The contributions from various emission sources may change, necessitating further estimation efforts. It should be emphasized that our study analyzes the current contributions from various sources, highlighting the substantial proportion attributable to non-exhaust $PM_{2.5}$ emissions.

3.5. Patterns of $PM_{2.5}$ emissions in different fleet electrification scenarios

We analyzed peak hourly $PM_{2.5}$ emission characteristics under four fleet electrification scenarios: 35%, 50%, 75%, and 100% penetration rates, covering LDPVs, HDPVs, LDTs, and HDTs. As shown in **Figure 10(a)**, $PM_{2.5}$ emissions gradually decrease with increasing fleet electrification. However, the emission reduction rate is lower than the electrification penetration rate. At penetration rates of 35%, 50%, 75%, and 100%, $PM_{2.5}$ emissions are reduced by 6.96%, 11.01%, 17.77%, and 24.53% respectively compared to the base scenario. **Figure 10(b)** reveals that non-exhaust $PM_{2.5}$ emissions constitute a prominent proportion of the total emissions across all scenarios, reaching over 90%. This result indicates that without mitigation measures for non-exhaust sources, they may become the main contributor to traffic-related $PM_{2.5}$ pollution.

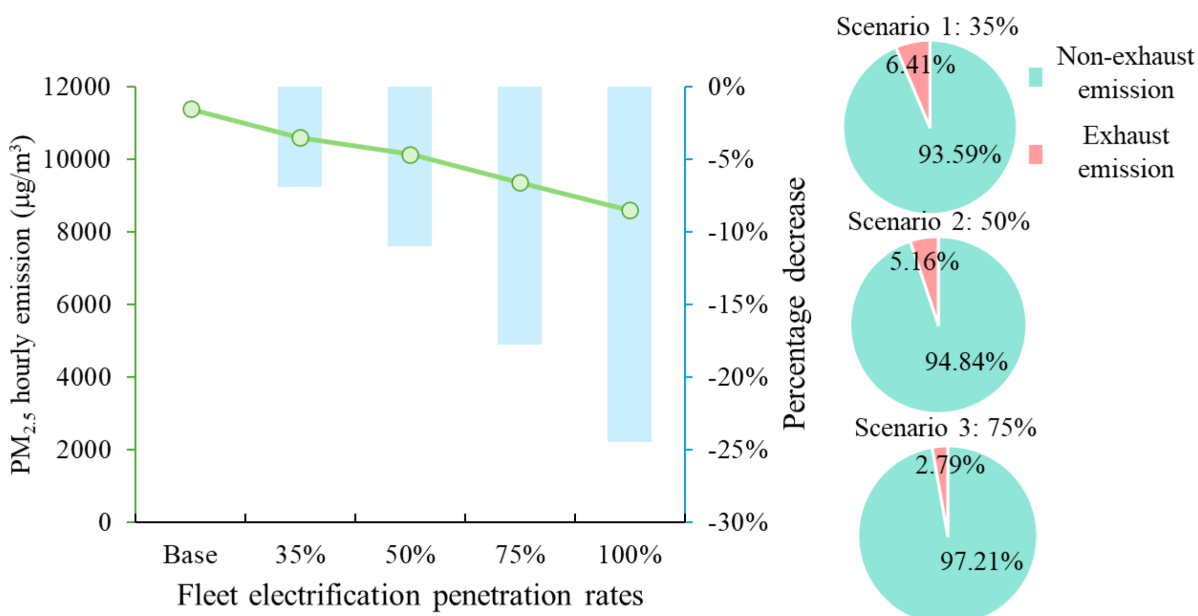

(a) (b)

Figure 10 $PM_{2.5}$ emissions patterns for different fleet electrification scenarios (EVs weight increases

by 20%, with the α value of 0.1). (a) Trends in total hourly emissions. (b) Characteristics of the share for exhaust and non-exhaust emissions.

These findings reveal a critical reality: fleet electrification cannot fully eliminate $PM_{2.5}$ emissions. Soret et al. (2014) also confirmed that even under high penetration scenarios, the reduction in $PM_{2.5}$ remains below 5%. **Table 3** shows studies by various researchers on the impact of vehicle fleet electrification on $PM_{2.5}$ emissions. A key point across studies is that the transition to EVs will not lead to a reduction in $PM_{2.5}$ emissions. The prevailing reality is that many countries are accelerating fleet electrification to achieve zero-pollution targets. Crucially, it must be emphasized that while EVs can achieve zero exhaust emissions, they do not equate to zero total emissions. This reality highlights the urgent need to shift the focus of next-phase traffic-related $PM_{2.5}$ control strategies toward non-exhaust emissions.

Moreover, the electrification of vehicle fleet may introduce new environmental justice concerns (Ji et al., 2015). The higher costs of EVs can create financial barriers for low-income populations (Adepetu and Keshav, 2017), who also face limited access to incentives for EVs purchase and charging (Min and Lee, 2020). Also, charging infrastructure is disproportionately concentrated in high-income neighborhoods (e.g., detached dwellings), severely limiting accessibility in disadvantaged communities (Hsu and Fingerman, 2021; Khan et al., 2022). Cangzhou exhibits this characteristic as well. Given that housing costs constitute a significant portion of household expenditure (Mirkatouli et al., 2018), housing price levels are frequently used to delineate communities of different socioeconomic status when census-level income data are unavailable (Coffee et al., 2013; Ding et al., 2023). Using housing price data obtained from Anjuke.com, we divided the study area into 1-km spatial grids. Grids with above-average housing prices were identified as affluent areas, while the remainder were classified as deprived areas.

More methodological details are available in our previously published research (Wang et al., 2025). The layout planning of charging infrastructure was obtained from the official website of the Cangzhou Municipal Government (https://www.cangzhou.gov.cn/cangzhou/). The charging facility density in both types of residential areas was calculated, with affluent areas exhibiting a higher charging facility coverage rate (65.75%), compared to only 16.49% in deprived areas (More details can be seen in our **Supplementary Materials**). This inequity hinders vehicle fleet electrification in disadvantaged communities and may result in concentrated exposure to exhaust emissions.

Additionally, the poorer living conditions in low-income communities (e.g., inadequate road maintenance or absence of green buffers) may lead to heightened pollution exposure from non-exhaust sources such as resuspended dust. We conducted a statistical analysis of housing price levels near various road types in Cangzhou. The results revealed that roads permitting truck traffic are associated with lower average surrounding housing prices (7,159 yuan/m^2), whereas other roads are flanked by residential areas with higher average prices (8,354 yuan/m^2). More details can be seen in our **Supplementary Materials**. As disadvantaged groups tend to seek more affordable housing, areas near truck-permitted roads and poorer environments often become their residential locations(Chakraborty et al., 2022; Li et al., 2025, 2018). Given that trucks are a major source of $PM_{2.5}$ emissions from exhaust and also generate higher non-exhaust emissions due to their heavier weight, residents in these areas are directly exposed to high $PM_{2.5}$ pollution, posing serious health risks to these communities. In contrast, the higher housing price communities feature better residential and green environments, and prohibit truck traffic, which enhances the capacity to capture and mitigate particulate matter. This unequal distribution of pollution exposure among population groups is a globally observed phenomenon (Demetillo et al., 2020; deSouza et al., 2023). Under the scenario of fleet electrification, non-exhaust emissions are becoming increasingly dominant, and the lack of attention to this shift may further widen disparities and bring new environmental justice challenges in $PM_{2.5}$ exposure across different demographic groups. Thus, the challenges arising from the complex interaction among vehicle-sourced $PM_{2.5}$ emissions, accelerated electrification, and evolving urban governance frameworks cannot be ignored, necessitating a shift in mitigation strategies.

Table 3 Some references about the impact of fleet electrification on $PM_{2.5}$ emissions.

References	City (Country)	Key points
Liu et al. (2024)	UK	By 2040, EVs are projected to contribute 98% of road transport $PM_{2.5}$ emissions.
Soret et al. (2014)	Barcelona and Madrid (Spain)	The high share of non-exhaust emissions has limited the $PM_{2.5}$ reduction from fleet electrification (< 8%).
Timmers and Achten (2016)	/	EVs may not significantly contribute to reducing $PM_{2.5}$ levels. Compared to ICEVs. EVs only reduce $PM_{2.5}$ emissions by 1–3%, and non-exhaust emissions already account for 85% of the total.
Liu et al. (2021)	/	The total particulate matter from an ICEV may be lower than the non-exhaust particulate emissions from its equivalent EV.
Grange et al. (2021)	Switzerland	Non-exhaust emissions are a significant contributor to the increase in $PM_{2.5}$ in the urban areas.
Fang et al. (2024)	Tianjin (China)	Non-exhaust emissions account for a growing share of vehicle emissions as the market share of EVs increases.
Zhang et al., (2025)	Tianjin (China)	Non-exhaust emissions from brake and tire wear surpassed exhaust emissions for the first time in 2013. Controlling these non-exhaust emissions is crucial for mitigating urban particulate matter pollution.
Acocella et al. (2025)	/	EVs do not substantially address non-exhaust emissions.
OECD (2020)	/	Heavier EVs (approximately 40% heavier) could lead to a 2.6–7.8% increase in $PM_{2.5}$ emissions.

4. Conclusions

In this study, a method for $PM_{2.5}$ emission estimation incorporating exhaust and non-exhaust sources from road networks was developed. Using Cangzhou, China as the case study, the method was validated with real $PM_{2.5}$ concentration data measured in roadside environment by a taxi-based mobile cruise sensing system, revealing emission patterns of road-network $PM_{2.5}$ in medium-sized populous cities in developing countries.

Non-exhaust $PM_{2.5}$ emissions now constitute a growing proportion of road traffic-related emissions. While past regulatory efforts have targeted exhaust emissions, a strategic shift in focus is urgently needed. It must be acknowledged that EVs are not zero-emission, and fleet electrification alone does not fully eliminate $PM_{2.5}$ pollution. Traffic-related $PM_{2.5}$ remains a critical environmental and public health issue, even amid the transition to electrification.

As non-exhaust emissions gain dominance, the continued neglect of these sources risks may exacerbate socioeconomic disparities and introduce new environmental justice concerns across demographic groups. Specifically, overlooking non-exhaust emissions may lead to significant underestimation of population exposure to traffic pollution. Evidence from Cangzhou, for example, indicates that disadvantaged groups often reside near truck-intensive corridors. A narrow focus on exhaust emissions alone would ignore the health risks posed by non-exhaust sources. Furthermore, uneven progress in electrification (e.g. higher charging infrastructure density in affluent areas) may slow the adoption of EVs in disadvantaged communities, leading to concentrated exposure to both exhaust and non-exhaust emissions in regions where electrification lags.

Innovative and multi-faceted strategies are needed to address traffic-related $PM_{2.5}$ emissions. While regulations such as the Euro 7 and China's upcoming China VII standards mark important high-level efforts to curb non-exhaust emissions, a more integrated and systematic approach is essential. Technologically, advancements in lightweight electric vehicle batteries should be prioritized, given the direct relationship between vehicle weight and non-exhaust emissions. It is critical to balance higher battery capacity (an increase that typically raises vehicle weight) against the associated rise in non-exhaust emissions. Concurrently, optimizing road surfaces and tire materials can reduce wear-related particulate release. Improved urban management and road maintenance, such as systematic street cleaning, use of dust suppressants, and selection of effective cleaning techniques, are also critical to limit dust resuspension. Additionally, modifying driver behavior offers a valuable complementary pathway. Training programs that emphasize eco-driving techniques over basic vehicle operation can mitigate aggressive driving styles that elevate emissions. Promoting regular maintenance of tire pressure and wheel alignment will further help reduce non-exhaust $PM_{2.5}$. Collectively, these all necessitate a fundamental evolution in emission governance strategies, shifting moves beyond the traditional singular focus on exhaust emissions toward an integrated framework that systematically addresses non-exhaust sources as the dominant contributor to $PM_{2.5}$ in the era of electric mobility.

There are still limitations in our study. Due to the high costs associated with measuring $PM_{2.5}$ non-exhaust emission factors, we employed model-based estimations derived from literature. Future studies could incorporate experimental measurements of non-exhaust emissions to expand the $PM_{2.5}$ emission factor database.

Acknowledgements

This work was supported by the Open Research Fund of Science and Technology Innovation Platform of Hunan Key Laboratory of Smart Roadway and Cooperative Vehicle-

Infrastructure Systems, Changsha University of Science & Technology [grant number kfj2508]; the National Natural Science Foundation of China [grant number 52272340]; Shandong Natural Science Foundation Innovation and Development Joint Fund [grant number ZR2024LZN008].

References

Acocella, M., Bianco, C., Tosco, T., Sethi, R., 2025. Mobility of non-exhaust brake wear dust from road traffic in saturated and unsaturated porous media mimicking subsurface environments. J Hazard Mater 491, 137851.

Adepetu, A., Keshav, S., 2017. The relative importance of price and driving range on electric vehicle adoption: Los Angeles case study. Transportation (Amst) 44, 353–373. https://doi.org/10.1007/s11116-015-9641-y

Amato, F., Cassee, F.R., Van Der Gon, H.A.D., Gehrig, R., Gustafsson, M., Hafner, W., Harrison, R.M., Jozwicka, M., Kelly, F.J., Moreno, T., 2014. Urban air quality: the challenge of traffic non-exhaust emissions. J Hazard Mater 275, 31–36.

Amato, F., Favez, O., Pandolfi, M., Alastuey, A., Querol, X., Moukhtar, S., Bruge, B., Verlhac, S., Orza, J.A.G., Bonnaire, N., Le Priol, T., Petit, J.-F., Sciare, J., 2016. Traffic induced particle resuspension in Paris: Emission factors and source contributions. Atmos Environ 129, 114–124. https://doi.org/https://doi.org/10.1016/j.atmosenv.2016.01.022

Apte, J.S., Messier, K.P., Gani, S., Brauer, M., Kirchstetter, T.W., Lunden, M.M., Marshall, J.D., Portier, C.J., Vermeulen, R.C.H., Hamburg, S.P., 2017. High-Resolution Air Pollution Mapping with Google Street View Cars: Exploiting Big Data. Environ Sci Technol 51, 6999–7008. https://doi.org/10.1021/acs.est.7b00891

Barlow, T., 2014. Briefing paper on non-exhaust particulate emissions from road transport. Transport Research Laboratory.

Beddows, D.C.S., Harrison, R.M., 2021. PM10 and PM2. 5 emission factors for non-exhaust particles from road vehicles: Dependence upon vehicle mass and implications for battery electric vehicles. Atmos Environ 244, 117886.

Beijing Municipal Ecology and Environment Bureau, 2018. The latest PM2.5 source apportionment analysis for Beijing [WWW Document]. URL https://sthjj.beijing.gov.cn/bjhrb/index/xxgk69/zfxxgk43/fdzdgknr2/ywdt28/xwfb/832588/index.html (accessed 5.8.25).

Berdegué, J.A., Soloaga, I., 2018. Small and medium cities and development of Mexican rural areas. World Dev 107, 277–288. https://doi.org/https://doi.org/10.1016/j.worlddev.2018.02.007

Bressi, S., Fiorentini, N., Huang, J., Losa, M., 2019. Crumb rubber modifier in road asphalt pavements: State of the art and statistics. Coatings 9, 384.

Burghardt, K., Uhl, J.H., Lerman, K., Leyk, S., 2022. Road network evolution in the urban and rural United States since 1900. Comput Environ Urban Syst 95, 101803. https://doi.org/https://doi.org/10.1016/j.compenvurbsys.2022.101803

Chakraborty, J., Collins, T.W., Grineski, S.E., Aun, J.J., 2022. Air pollution exposure disparities in US public housing developments. Sci Rep 12, 9887.

Chen, H., Kwong, J.C., Copes, R., Tu, K., Villeneuve, P.J., Van Donkelaar, A., Hystad, P., Martin, R. V, Murray, B.J., Jessiman, B., 2017. Living near major roads and the incidence of dementia, Parkinson’s disease, and multiple sclerosis: a population-based cohort study. The Lancet 389, 718–726.

Chen, Y., Li, S., Pan, Y., Zhang, J., 2022. Urban expressway congestion forewarning based on slope change of traffic flow fundamental diagram. J Transp Eng A Syst 148, 04022030.

Coffee, N.T., Lockwood, T., Hugo, G., Paquet, C., Howard, N.J., Daniel, M., 2013. Relative residential property value as a socio-economic status indicator for health research. Int J Health Geogr 12, 1–10.

Dabek-Zlotorzynska, E., Celo, V., Ding, L., Herod, D., Jeong, C.-H., Evans, G., Hilker, N., 2019. Characteristics and sources of PM2.5 and reactive gases near roadways in two metropolitan areas in Canada. Atmos Environ 218, 116980. https://doi.org/https://doi.org/10.1016/j.atmosenv.2019.116980

De Coensel, B., Can, A., Degraeuwe, B., De Vlieger, I., Botteldooren, D., 2012. Effects of traffic signal coordination on noise and air pollutant emissions. Environmental Modelling & Software 35, 74–83.

Demetillo, M.A.G., Navarro, A., Knowles, K.K., Fields, K.P., Geddes, J.A., Nowlan, C.R., Janz, S.J., Judd, L.M., Al-Saadi, J., Sun, K., McDonald, B.C., Diskin, G.S., Pusede, S.E., 2020. Observing Nitrogen Dioxide Air Pollution Inequality Using High-Spatial-Resolution Remote Sensing Measurements in Houston, Texas. Environ Sci Technol 54, 9882–9895. https://doi.org/10.1021/acs.est.0c01864

deSouza, P.N., Chaudhary, E., Dey, S., Ko, S., Németh, J., Guttikunda, S., Chowdhury, S., Kinney, P., Subramanian, S. V, Bell, M.L., 2023. An environmental justice analysis of air pollution in India. Sci Rep 13, 16690.

Ding, Y., Wang, C., Wang, J., Wang, P., Huang, L., 2023. Revealing the impact of built environment, air pollution and housing price on health inequality: an empirical analysis of Nanjing, China. Front Public Health 11, 1153021.

EEA, 2022. Emissions of air pollutants from transport in Europe [WWW Document]. URL https://www.eea.europa.eu/en/analysis/indicators/emissions-of-air-pollutants-from (accessed 10.16.25).

Fang, T., Fu, J., Gao, Y., Song, A., Zhang, Y., Zhang, Q., Wu, L., Peng, J., Wang, T., Mao, H., 2024. Real-world vehicular source indicators for exhaust and non-exhaust contribution to PM2. 5 during peak and off-peak hours using tunnel measurement. Journal of Geophysical Research: Atmospheres 129, e2024JD040853.

Faria, R., Moura, P., Delgado, J., De Almeida, A.T., 2012. A sustainability assessment of electric vehicles as a personal mobility system. Energy Convers Manag 61, 19–30.

Fussell, J.C., Franklin, M., Green, D.C., Gustafsson, M., Harrison, R.M., Hicks, W., Kelly, F.J., Kishta, F., Miller, M.R., Mudway, I.S., 2022. A review of road traffic-derived non-exhaust particles: emissions, physicochemical characteristics, health risks, and mitigation measures. Environ Sci Technol 56, 6813–6835.

Garg, B.D., Cadle, S.H., Mulawa, P.A., Groblicki, P.J., Laroo, C., Parr, G.A., 2000. Brake wear particulate matter emissions. Environ Sci Technol 34, 4463–4469.

Giechaskiel, B., Grigoratos, T., Mathissen, M., Quik, J., Tromp, P., Gustafsson, M., Franco, V., Dilara, P., 2024. Contribution of road vehicle tyre wear to microplastics and ambient air pollution. Sustainability 16, 522.

Grange, S.K., Fischer, A., Zellweger, C., Alastuey, A., Querol, X., Jaffrezo, J.-L., Weber, S., Uzu, G., Hueglin, C., 2021. Switzerland's PM10 and PM2. 5 environmental increments show the importance of non-exhaust emissions. Atmos Environ X 12, 100145.

Gulia, S., Goyal, P., Goyal, S.K., Kumar, R., 2019. Re-suspension of road dust: contribution, assessment and control through dust suppressants—a review. International Journal of Environmental Science and Technology 16, 1717–1728.

Gummeneni, S., Yusup, Y. Bin, Chavali, M., Samadi, S.Z., 2011. Source apportionment of particulate matter in the ambient air of Hyderabad city, India. Atmos Res 101, 752–764.

Halonen, J.I., Blangiardo, M., Toledano, M.B., Fecht, D., Gulliver, J., Anderson, H.R., Beevers, S.D., Dajnak, D., Kelly, F.J., Tonne, C., 2016. Long-term exposure to traffic pollution and hospital admissions in London. Environmental Pollution 208, 48–57. https://doi.org/https://doi.org/10.1016/j.envpol.2015.09.051

Hooftman, N., Messagie, M., Joint, F., Segard, J.-B., Coosemans, T., 2018. In-life range modularity for electric vehicles: The environmental impact of a range-extender trailer system. Applied Sciences 8, 1016.

Houbraken, M., Logghe, S., Audenaert, P., Colle, D., Pickavet, M., 2018. Examining the potential of floating car data for dynamic traffic management. IET Intelligent Transport Systems 12, 335–344.

Hsu, C.-W., Fingerman, K., 2021. Public electric vehicle charger access disparities across race and income in California. Transp Policy (Oxf) 100, 59–67. https://doi.org/https://doi.org/10.1016/j.tranpol.2020.10.003

Jeong, C.-H., Wang, J.M., Hilker, N., Debosz, J., Sofowote, U., Su, Y., Noble, M., Healy, R.M., Munoz, T., Dabek-Zlotorzynska, E., 2019. Temporal and spatial variability of traffic-related PM2. 5 sources: Comparison of exhaust and non-exhaust emissions. Atmos Environ 198, 55–69.

Ji, S., Cherry, C.R., Zhou, W., Sawhney, R., Wu, Y., Cai, S., Wang, S., Marshall, J.D., 2015. Environmental justice aspects of exposure to PM2. 5 emissions from electric vehicle use in China. Environ Sci Technol 49, 13912–13920.

Jiang, Y., Song, G., Zhang, Z., Zhai, Z., Yu, L., 2021. Estimation of hourly traffic flows from floating car data for vehicle emission estimation. J Adv Transp 2021, 6628335.

Karner, A., Golub, A., 2019. Assessing the equity impacts of a transportation investment program, in: Measuring Transport Equity. Elsevier, pp. 277–290.

Kendrick, C.M., Koonce, P., George, L.A., 2015. Diurnal and seasonal variations of NO, NO2 and PM2. 5 mass as a function of traffic volumes alongside an urban arterial. Atmos Environ 122, 133–141.

Khan, H.A.U., Price, S., Avraam, C., Dvorkin, Y., 2022. Inequitable access to EV charging infrastructure. The Electricity Journal 35, 107096. https://doi.org/https://doi.org/10.1016/j.tej.2022.107096

Kwak, J., Kim, H., Lee, J., Lee, S., 2013. Characterization of non-exhaust coarse and fine particles from on-road driving and laboratory measurements. Science of the Total Environment 458, 273–282.

Lewis, A., Moller, S.J., Carslaw, D., 2019. Non-Exhaust Emissions from Road Traffic.

Li, B., Fan, C., Chien, Y.-H., Mostafavi, A., 2025. Human mobility disproportionately extends PM2. 5 emission exposure for low income populations. Sustain Cities Soc 119, 106063.

Li, C., Managi, S., 2021. Contribution of on-road transportation to PM2. 5. Sci Rep 11, 21320.

Li, M., Wang, K., Xiong, Y., 2021. Multiple intermolecular interaction to improve the abrasion resistance and wet skid resistance of eucommia ulmoides gum/styrene butadiene rubber composite. Materials 14, 5246.

Li, V.O.K., Han, Y., Lam, J.C.K., Zhu, Y., Bacon-Shone, J., 2018. Air pollution and environmental injustice: Are the socially deprived exposed to more PM2. 5 pollution in Hong Kong? Environ Sci Policy 80, 53–61.

Lin, S., Liu, Y., Chen, H., Wu, S., Michalaki, V., Proctor, P., Rowley, G., 2022. Impact of change in traffic flow on vehicle non-exhaust PM2. 5 and PM10 emissions: A case study of the M25 motorway, UK. Chemosphere 303, 135069.

Liu, J., Han, K., Chen, X.M., Ong, G.P., 2019. Spatial-temporal inference of urban traffic emissions based on taxi trajectories and multi-source urban data. Transp Res Part C Emerg Technol 106, 145–165.

Liu, J., Ma, T., Chen, J., Peng, X., Zhang, Y., Wang, Y., Peng, J., Shi, G., Wei, Y., Gao, J., 2024. Insights into PM2. 5 pollution of four small and medium-sized cities in Chinese representative regions: Chemical compositions, sources and health risks. Science of The Total Environment 918, 170620.

Liu, Y., Chen, H., Gao, J., Li, Y., Dave, K., Chen, J., Federici, M., Perricone, G., 2021. Comparative analysis of non-exhaust airborne particles from electric and internal combustion engine vehicles. J Hazard Mater 420, 126626.

Liu, Y., Chen, H., Jiang, L., Li, T., Guo, J., Wei, T., Crowther, R., 2024. Environmental and health impacts of banning passenger cars with internal combustion engines: A case study of Leeds, UK. Transp Res D Transp Environ 134, 104343.

Liu, Y., Chen, H., Li, Y., Gao, J., Dave, K., Chen, J., Li, T., Tu, R., 2022a. Exhaust and non-exhaust emissions from conventional and electric vehicles: A comparison of monetary impact values. J Clean Prod 331, 129965.

Liu, Y., Chen, H., Wu, S., Gao, J., Li, Y., An, Z., Mao, B., Tu, R., Li, T., 2022b. Impact of vehicle type, tyre feature and driving behaviour on tyre wear under real-world driving conditions. Science of The Total Environment 842, 156950. https://doi.org/https://doi.org/10.1016/j.scitotenv.2022.156950

Masiol, M., Hopke, P.K., Felton, H.D., Frank, B.P., Rattigan, O. V, Wurth, M.J., LaDuke, G.H., 2017. Source apportionment of PM2. 5 chemically speciated mass and particle number concentrations in New York City. Atmos Environ 148, 215–229.

Masri, S., Kang, C.-M., Koutrakis, P., 2015. Composition and sources of fine and coarse particles collected during 2002–2010 in Boston, MA. J Air Waste Manage Assoc 65, 287–297.

Matthaios, V.N., Lawrence, J., Martins, M.A.G., Ferguson, S.T., Wolfson, J.M., Harrison, R.M., Koutrakis, P., 2022. Quantifying factors affecting contributions of roadway exhaust and non-exhaust emissions to ambient PM10–2.5 and PM2.5–0.2 particles. Science of The Total Environment 835, 155368. https://doi.org/https://doi.org/10.1016/j.scitotenv.2022.155368

Min, Y., Lee, H.W., n.d. Social Equity of Clean Energy Policies in Electric-Vehicle Charging Infrastructure Systems, in: Construction Research Congress 2020. pp. 221–229. https://doi.org/10.1061/9780784482858.025

Ministry of Ecology and Environment of the People's Republic of China (MEEC), 2019. China mobile source environmental management annual report 2019.

Mirkatouli, J., Samadi, R., Hosseini, A., 2018. Evaluating and analysis of socio-economic variables on land and housing prices in Mashhad, Iran. Sustain Cities Soc 41, 695–705.

OECD, 2020. Non-exhaust Particulate Emissions from Road Transport: An Ignored Environmental Policy Challenge. https://doi.org/https://doi.org/10.1787/4a4dc6ca-en

Pan, Y., Cheng, Q., Li, A., Zhang, J., Guo, J., Chen, Y., 2024. Analysis of congestion key parameters, dynamic discharge process, and capacity estimation at urban freeway bottlenecks: a case study in Beijing, China. Transportation Letters 1–20.

Philip K. Hopke, 2022. PM2.5 Source Apportionment of Major Cities in Asia [WWW Document]. URL http://www.allaboutair.cn/uploads/soft/230817/PM2.5SourceApportionmentAsiaEN.pdf (accessed 5.8.25).

Piscitello, A., Bianco, C., Casasso, A., Sethi, R., 2021a. Non-exhaust traffic emissions: Sources, characterization, and mitigation measures. Science of the Total Environment 766, 144440.

Piscitello, A., Bianco, C., Casasso, A., Sethi, R., 2021b. Non-exhaust traffic emissions: Sources, characterization, and mitigation measures. Science of The Total Environment 766, 144440. https://doi.org/https://doi.org/10.1016/j.scitotenv.2020.144440

Querol, X., Amato, F., Robusté, F., Holman, C., Harrison, R.M., 2018. Non-technological measures on road traffic to abate urban air pollution, in: Non-Exhaust Emissions. Elsevier, pp. 229–260.

Ramacher, M.O.P., Matthias, V., Aulinger, A., Quante, M., Bieser, J., Karl, M., 2020. Contributions of traffic and shipping emissions to city-scale NOx and PM2. 5 exposure in Hamburg. Atmos Environ 237, 117674.

Ratanavalachai, T., Trivitayanurak, W., 2023. Application of a PM2. 5 dispersion model in the Bangkok central business district for air quality management. Front Environ Sci 11, 1237366.

Razo, D.A.S., Decrock, J., Opsommer, A., Fabré, M., Persoon, F., 2016. Promaxon® D in NAO Non steel disc Pad formulations: the importance in the third body layer and its effect on brake noise. SAE International Journal of Materials and Manufacturing 9, 158–170.

Rowangould, G.M., 2015. A new approach for evaluating regional exposure to particulate matter emissions from motor vehicles. Transp Res D Transp Environ 34, 307–317.

Rowangould, G.M., 2013. A census of the US near-roadway population: Public health and environmental justice considerations. Transp Res D Transp Environ 25, 59–67. https://doi.org/https://doi.org/10.1016/j.trd.2013.08.003

Salva, J., Vanek, M., Schwarz, M., Gajtanska, M., Tonhauzer, P., Ďuricová, A., 2021. An assessment of the on-road mobile sources contribution to particulate matter air pollution by AERMOD dispersion model. Sustainability 13, 12748.

Shenzhen Municipal Ecology and Environment Bureau, 2015. Motor vehicles are the predominant source of PM2.5 pollution in Shenzhen [WWW Document]. URL https://meeb.sz.gov.cn/xxgk/qt/hbyw/dqzlgl/content/post_2040225.html (accessed 5.8.25).

Shi, G., Shan, J., Ding, L., Ye, P., Li, Y., Jiang, N., 2019. Urban road network expansion and its driving variables: a case study of Nanjing City. Int J Environ Res Public Health 16, 2318.

Soleimani, M., Akbari, N., Saffari, B., Haghshenas, H., 2022. Health effect assessment of PM2.5 pollution due to vehicular traffic (case study: Isfahan). J Transp Health 24, 101329. https://doi.org/https://doi.org/10.1016/j.jth.2022.101329

Soret, A., Guevara, M., Baldasano, J.M., 2014. The potential impacts of electric vehicles on air quality in the urban areas of Barcelona and Madrid (Spain). Atmos Environ 99, 51–63.

Sunderrajan, A., Viswanathan, V., Cai, W., Knoll, A., 2016. Traffic state estimation using floating car data. Procedia Comput Sci 80, 2008–2018.

Tian, Y., Wang, A., Mora, S., deSouza, P., Yao, X., Duarte, F., Lin, H., Ratti, C., 2023. Improving NO2 prediction by integrating tree diversity, urban form, and scale sensitivity through mobile monitoring. Applied Geography 154, 102943. https://doi.org/https://doi.org/10.1016/j.apgeog.2023.102943

Timmers, V.R.J.H., Achten, P.A.J., 2016. Non-exhaust PM emissions from electric vehicles. Atmos Environ 134, 10–17.

Tomar, G., Nagpure, A.S., Kumar, V., Jain, Y., 2022. High resolution vehicular exhaust and non-exhaust emission analysis of urban-rural district of India. Science of The Total Environment 805, 150255.

Vieira, T., Lundberg, J., Genell, A., Sandberg, U., Blomqvist, G., Gustafsson, M., Janhäll, S., Erlingsson, S., 2019. Porous pavement for reduced tyre/road noise and improved air quality-initial results from a case study, in: Proceedings of the 26th International Congress on Sound and Vibration, ICSV.

Vojtíšek-Lom, M., Vaculík, M., Pechout, M., Hopan, F., Arul Raj, A.F., Penumarti, S., Horák, J.S., Popovicheva, O., Ondráček, J., Doušová, B., 2021. Effects of braking conditions on nanoparticle emissions from passenger car friction brakes. Science of The Total Environment 788, 147779. https://doi.org/https://doi.org/10.1016/j.scitotenv.2021.147779

Wang, F., Peng, Y., Jiang, C., 2017. Influence of road patterns on PM2. 5 concentrations and the available solutions: The case of Beijing City, China. Sustainability 9, 217.

Wang, L., Jiang, L., Zhai, Z., Yu, L., Song, G., Wu, Y., 2025. Are deprived communities exposed to higher PM2. 5 concentrations? Evidence from Cangzhou, China. Transp Res D Transp Environ 143, 104762.

Wang, Q., Liu, M., Yu, Y., Li, Y., 2016. Characterization and source apportionment of PM2. 5-bound polycyclic aromatic hydrocarbons from Shanghai city, China. Environmental Pollution 218, 118–128.

Wang, S., Yu, D., Kwan, M.-P., Zheng, L., Miao, H., Li, Y., 2020. The impacts of road network density on motor vehicle travel: An empirical study of Chinese cities based on network theory. Transp Res Part A Policy Pract 132, 144–156. https://doi.org/https://doi.org/10.1016/j.tra.2019.11.012

Wang, S., Yu, D., Kwan, M.-P., Zhou, H., Li, Y., Miao, H., 2019. The evolution and growth patterns of the road network in a medium-sized developing city: a historical investigation of Changchun, China, from 1912 to 2017. Sustainability 11, 5307.

Wei, N., Jia, Z., Men, Z., Ren, C., Zhang, Y., Peng, J., Wu, L., Wang, T., Zhang, Q., Mao, H., 2022. Machine learning predicts emissions of brake wear PM2. 5: model construction and interpretation. Environ Sci Technol Lett 9, 352–358.

Wu, Y., Wang, Y., Wang, L., Song, G., Gao, J., Yu, L., 2020. Application of a taxi-based mobile atmospheric monitoring system in Cangzhou, China. Transp Res D Transp Environ 86, 102449.

Xu, L., Yue, Y., Li, Q., 2013. Identifying urban traffic congestion pattern from historical floating car data. Procedia-Social and Behavioral Sciences 96, 2084–2095.

Yu, C., Deng, Y., Qin, Z., Yang, C., Yuan, Q., 2023. Traffic volume and road network structure: Revealing transportation-related factors on PM2.5 concentrations. Transp Res D Transp Environ 124, 103935. https://doi.org/https://doi.org/10.1016/j.trd.2023.103935

Yu, Y.T., Xiang, S., Zhang, T., You, Y., Si, S., Zhang, S., Wu, Y., 2022. Evaluation of City-Scale Disparities in PM2. 5 Exposure Using Hyper-Localized Taxi-Based Mobile Monitoring. Environ Sci Technol 56, 13584–13594.

Zang, J., Jiao, P., Song, G., Li, Z., Peng, T., 2022. A Novel Environment Estimation Method of Whole Sample Traffic Flows and Emissions Based on Multifactor MFD. Int J Environ Res Public Health 19, 16524.

Zhang, B., Cheng, S., Zhao, Y., Lu, F., 2024. Health impacts of spatiotemporal variation in PM2. 5 concentrations from heavy-duty diesel trucks in Beijing. J Clean Prod 434, 140025.

Zhang, Q., Fang, T., Yin, J., Men, Z., Peng, J., Wu, L., Mao, H., 2025. Vehicle non-exhaust emissions significantly contribute to urban PM pollution in new energy vehicles era. Journal of Geophysical Research: Atmospheres 130, e2024JD042126.

Zhao, N., Yu, L., Zhao, H., Guo, J., Wen, H., 2009. Analysis of traffic flow characteristics on ring road expressways in Beijing: Using floating car data and remote traffic microwave sensor data. Transp Res Rec 2124, 178–185.

Zum Hagen, F.H.F., Mathissen, M., Grabiec, T., Hennicke, T., Rettig, M., Grochowicz, J., Vogt, R., Benter, T., 2019. Study of brake wear particle emissions: impact of braking and cruising conditions. Environ Sci Technol 53, 5143–5150.